

Nonsingular Wormhole with an anisotropic matter

Hyeong-Chan Kim,^a Youngone Lee^{a,1}

^aSchool of Liberal Arts and Sciences, Korea National University of Transportation, Chungju 380-702, Korea

E-mail: hyeongchan@gmail.com, youngone@ut.ac.kr

Abstract. We study the geometry of a spacetime having a wormhole in the context of general relativity and find new static and spherically-symmetric solutions, exact and numerical ones. The spacetime consists of anisotropic matter. We specify the existence condition for a wormhole throat. We analyze properties of the solutions after categorizing them based on the spacetime regularity and signature of energy density. We describe the physical conditions that make the spacetime nonsingular.

¹Corresponding author.

Contents

1	Introduction	1
2	General Properties and Existence Conditions	2
2.1	Tolmann-Oppenheimer-Volkhoff equation	3
2.2	The existence condition for a wormhole ‘throat’	4
3	Analysis for general solutions	5
3.1	Analysis for $w_1 < -1$	7
3.2	Analysis for $w_1 > 0$	7
3.3	behaviors around important points	8
3.3.1	The asymptotic behavior around \mathcal{O}	8
3.3.2	Behavior of around a wormhole ‘throat’ P_T	9
3.3.3	behavior around the bouncing point P_B	10
4	Numerical solutions	11
4.1	$w_1 < -1$ case	11
4.2	$w_1 > 0$ case	12
5	Exactly solvable cases	13
5.1	Specific solution for the case $1 + w_1 + 2w_2 = 0$	13
5.2	Various solutions for case $1 + w_1 + 4w_2 = 0$	14
6	Special Solutions	15
6.1	Perturbative solution for $1 + w_1 + 2w_2 = 0$ case	15
6.2	Limiting solution for $ s \gg 1$	16
7	Summary and Discussions	18

1 Introduction

Wormhole spacetime is a solution of general relativity [1–3] which differ from other solutions such as massive stars and black holes. The key difference is the topology. Two asymptotic regions are connected by a passage called a ‘throat’. Since general relativity is a local theory, it does not tell what the topology of whole spacetime should be and does not exclude wormhole spacetimes.

Although wormholes are genuine solutions of general relativity, the study of wormholes had not drawn much interest of researchers until recently. The main reason is that the existence of wormhole requires violation of energy conditions, which are strong requirements to matter based on human intuitions on ordinary classical matter. To pass a ‘throat’ of a wormhole, the geodesics of light bundle converge and then diverge which requires ‘exotic’ or ‘phantom’ matter having negative energy density [2, 4]. Another reason is that this unique topology obscures many previously accepted concepts. One may construct a time machine [2, 5], may have ‘charge without charge’ [6] and the ADM mass measured in one side of the wormhole may not be identical to that in the other side [5, 7].

Despite of this pathology, researchers in this field have studied wormholes as physical objects in the hope of future resolution of energy conditions. Recently, an attempt to construct ‘phantom free models’ was suggested [10] while others have tried to get around the pathology by constructing a wormhole using ‘ordinary’ matter in modified theories of gravity [11–15]. On the other hand, in quantum world, many examples were found which allow the violation of energy conditions. Casimir effect [8], negative energy region of squeezed light [9] and the dark energy are the most prominent examples. Therefore, it is possible to accept the violation of the energy condition for a special circumstance in general relativity.

Recently, wormholes have drawn interests as a test-bed to understand quantum entanglement. A non-traversable wormhole is regarded as a pair of entangled black holes in ‘ER=EPR’ conjecture to understand the information paradox [16]. Traversable wormholes have been also suggested to have physically sensible interpretation of the conjecture [17]. The study of wormholes as physical entities in understanding the quantum-gravity era is getting more important than ever at this juncture.

Our purpose in this paper is, as a preliminary step, to categorize nonsingular wormhole solutions and study the characteristic features of those solutions to attain more clear grasp of the physical aspects of wormholes. We focus on static, spherically symmetric traversable wormholes which consist of anisotropic matter in the context of general relativity. The anisotropic matter we are considering here satisfies linear equation of state throughout the entire space. Hence isotropic perfect fluids are a special case of our study. Although the anisotropic matter is distributed throughout the entire space, one can obtain a spacetime of desirable asymptotic properties or of minimal ‘exotic’ matter with appropriate junction conditions to match a truncated solution of us [18].

Traditionally a wormhole solution is obtained by assuming a well-behaved wormhole metric first and calculate the Riemann tensor to get an appropriate stress-energy tensor for matter field afterward [19]. On the other hand, in this work, we begin with the specification of the matter satisfying a given equations of state and then solve Einstein’s equation. After that, we find out the condition for a wormhole solution to be nonsingular over the whole spacetime. We also analyze the properties satisfied by the general solutions and categorize them into six types based on the spacetime regularity and signature of energy density.

The existence condition and properties of nonsingular wormhole solutions are discussed in Sec. 2. Analysis of general solutions is in Sec. 3 where behavior of solutions around special points such as points at asymptotes, the ‘throat’, the bouncing point will be analyzed. Numerical solutions are also presented in Sec. 4 and a few exact solutions are presented in Sec. 5. Properties of a specific solution with the case $1+w_1+2w_2=0$ and of limiting solutions are discussed in Sec. 6. Finally, we summarize the results and discuss the properties of the solutions and suggest future works to be done in Sec. 7.

2 General Properties and Existence Conditions

For simplicity, we consider the static and spherically symmetric configurations. The stress tensor for an anisotropic fluid compatible with the spherical symmetry is given by

$$T^{\mu\nu} = \rho u^\mu u^\nu + p_1 r^\mu r^\nu + p_2 (\theta^\mu \theta^\nu + \phi^\mu \phi^\nu), \quad (2.1)$$

where ρ is the energy density measured by a comoving observer with the fluid, the vectors are mutually orthogonal and u^μ is its four-velocity and r^μ is radial and θ^μ, ϕ^μ denote the unit

angular vectors, respectively. As we mentioned above, the radial and the angular pressures are assumed to be proportional to the density:

$$p_1 = w_1 \rho, \quad p_2 = w_2 \rho, \quad (2.2)$$

with constant w_1 and w_2 . We focus on a static-spherically symmetric configuration of which the line element¹ is given by

$$ds^2 = -f(r)dt^2 + \frac{1}{1 - 2m(r)/r}dr^2 + r^2 d\theta^2 + r^2 \sin^2 \theta d\phi^2. \quad (2.3)$$

2.1 Tolmann-Oppenheimer-Volkhoff equation

The G_{tt} part of the Einstein equation defines the mass function $m(r)$ as,

$$m(r) = 4\pi \int^r r'^2 \rho(r') dr', \quad (2.4)$$

where an integration constant is absorbed into the definition of $m(r)$. The continuity equation $\nabla^\mu T_{\mu\nu} = 0$ yields the Tolmann-Oppenheimer-Volkhoff (TOV) equation for an anisotropic matter,

$$p_1' = -(\rho + p_1) \frac{m + 4\pi r^3 p_1}{r(r - 2m)} + \frac{2(p_2 - p_1)}{r}. \quad (2.5)$$

Here the prime represents a derivative with respect to r .

Then g_{tt} part of the metric, or $f(r)$, can be obtained in two different ways. From the relation $G_{tt} = 8\pi T_{tt}$ we have

$$\frac{f'}{f} = \frac{2(m + 4\pi r^3 p_1)}{r(r - 2m)}. \quad (2.6)$$

The equation can be directly integrated to give

$$f(r) = \tilde{f}_0 \frac{(r - 2m)^{-w_1}}{r} \exp \left[(1 + w_1) \int_{r_0}^r \frac{1}{r - 2m(r)} dr \right], \quad (2.7)$$

where \tilde{f}_0 is an integration constant. Note that w_2 -dependence in (2.7) will be restored when $m(r)$ is expressed explicitly. The sign of \tilde{f}_0 will be chosen so that the signature of the metric be Lorentzian because the Einstein equation does not determine the sign of $f(r)$. On the other hand, the anisotropic TOV equation (2.5) with the equation of state (2.2) reads

$$\frac{\rho'}{\rho} = -\frac{1 + w_1}{2w_1} \frac{f'}{f} + \frac{2(w_2 - w_1)}{w_1} \frac{1}{r}.$$

After integrating one gets,

$$f(r) = f_0 \left(\frac{r}{r_0} \right)^{\frac{4(w_2 - w_1)}{(1 + w_1)}} \left(\frac{\rho}{\rho_0} \right)^{-\frac{2w_1}{1 + w_1}}, \quad (2.8)$$

where r_0 and ρ_0 is some referential values of size and density to be identified later and f_0 should be determined by matching $f(r)$ at $r = r_0$ with Eq. (2.7). We have two forms of $f(r)$, (2.7) and (2.8), and both are useful for later considerations.

¹Because we deal with spherically symmetric situation, many parts of the calculation in this section overlaps with those in Ref. [20]. Therefore, we leave only the main results.

The remaining task is to find the explicit form of $m(r)$ by solving the TOV equation². With respect to $m(r)$, using Eqs. (2.2) and (2.4), the TOV equation becomes,

$$\frac{m''}{m'} = -\frac{1+w_1}{2w_1} \frac{1+2w_1 m'}{r-2m} + \frac{1+w_1+4w_2}{2w_1 r}, \quad (2.9)$$

where we use $\rho'/\rho = m''/m' - 2/r$. Equation (2.9) does not allow an analytic solution in general. However, the above relation can be cast into a first order autonomous equation in a two dimensional (u, v) plane:

$$\frac{du}{dv} = \frac{-1}{1+w_1} \frac{(1-u)(2v-u)}{v[v-v_T+s(1-u)]}, \quad (2.10)$$

where u and v are scale-invariant variables defined by

$$u \equiv \frac{2m(r)}{r}, \quad v \equiv \frac{dm(r)}{dr} = 4\pi r^2 \rho. \quad (2.11)$$

The metric g_{tt} can be reconstructed from v via Eq. (2.8) and g_{rr} from u respectively.

The constants v_T and s represent the value of v at the wormhole ‘throat’ and the *slope* of the line $v - v_T + s(1 - u) = 0$, respectively,

$$v_T \equiv -\frac{1}{2w_1}, \quad s \equiv -\frac{1+w_1+4w_2}{2w_1(1+w_1)}. \quad (2.12)$$

2.2 The existence condition for a wormhole ‘throat’

Assume that a ‘throat’ of a wormhole forms at $r = r_T$, each side of which geometry is described by the metric (2.3) with appropriate mass function. For the metric (2.3) to have a ‘throat’ at $r = r_T$, its spatial part should have a coordinate singularity of the form $g_{rr} \approx g(1 - r_T/r)^{-1}$ with $g > 0$ where r is an areal radial coordinate³. We then find $f(r)$ from Eq. (2.7), to get

$$f(r) \propto \frac{g^{w_1}}{r} (r - r_T)^{(1+w_1)g-w_1}.$$

At the wormhole ‘throat’, $f(r_T)$ should take a finite value, hence the value of g to be

$$g \equiv \lim_{r \rightarrow r_T} \left(1 - \frac{r_T}{r}\right) g_{rr} = \frac{w_1}{1+w_1} > 0.$$

Therefore, a wormhole solution exists only when $w_1 < -1$ or $w_1 > 0$.⁴ Around the ‘throat’, the mass function $m(r)$ behaves as

$$m(r) \simeq \frac{r_T}{2w_1} \left(1 + w_1 - \frac{r}{r_T}\right) \Rightarrow m'(r_T) = -\frac{1}{2w_1}. \quad (2.13)$$

²When $w_1 = -1$ and $w_1 = -1/3 = w_2$, the TOV equation allows exact solutions as in Ref. [21, 22].

³Consider $g_{rr} \approx g(1 - r_T/r)^{-\beta}$. When $\beta < 1, \neq 0$, the geometry must be singular [20]. When $\beta \geq 2$, the geometry at $r = r_T$ can be regular but the surface $r = r_T$ is located at infinity implying that the ‘throat’ is non-traversable. Therefore, to be a traversable, the value should satisfy $1 \leq \beta < 2$. However, when β is non-integer, higher curvatures must have a singularity at $r = r_T$. In this sense, we restrict our interest to $\beta = 1$ case to find a nonsingular traversable wormhole.

⁴When $w_1 = 0$ and $g = 0$, the spatial geometry does not form a ‘throat’ at r_T . The solution for $w_1 = -1$ was analyzed in Ref. [22] thoroughly in which no wormhole-like solutions were found.

From this, one can see that the value of $v \equiv m'(r)$ at the wormhole ‘throat’ is solely determined by w_1 ⁵. Previous definition of $v_T (= -1/2w_1)$ comes from this observation.

Based on the observation above, let us divide the wormhole ‘throats’ into two cases:

1. When $w_1 > 0$ ($v_T < 0$): the mass function decreases from $r_T/2$ with r , meaning that mass inside the region ($r_T, R > r_T$) is $\Delta m = m(R) - m(r_T) < 0$. The energy density at the ‘throat’ takes a negative value $\rho(r_T) = v_T/4\pi r_T^2 < 0$.
2. When $w_1 < -1$ ($0 < v_T < 1/2$): the mass function increases with r and the density takes a positive value. Therefore, if we use matter with positive energy density to weave a wormhole ‘throat’, we cannot avoid phantom-like matter satisfying $w_1 < -1$.

As we previously commented, we consider nonsingular solutions in which all quantities are continuous throughout the entire spacetime. Thus, if necessary, solutions with a surface layer or discontinuous energy of a hypersurface [18] can be obtained by cut and paste our solutions with appropriate junction conditions. To express both sides of the ‘throat’ continuously, one may introduce a new radial coordinate x around the ‘throat’,

$$\sqrt{g_{rr}(r)}dr = \pm r_T dx \quad \Rightarrow \quad \pm x \simeq 2\sqrt{g}\sqrt{\frac{r}{r_T} - 1}, \quad (2.14)$$

where we choose $x = 0$ at the ‘throat’ and \pm for $x \gtrless 0$, respectively. This gives

$$\frac{dm(x)}{dx} = \frac{dr(x)}{dx}m'(r) = \frac{-(1+w_1)}{4w_1^2}x.$$

Therefore, there is no singularity of density at the wormhole ‘throat’. Note that the existence condition for a wormhole ‘throat’ is independent of the angular pressure.

3 Analysis for general solutions

The solution to the autonomous equation (2.10) can be denoted by an integral curve C on the two dimensional plane (u, v) . Hence, to sketch general properties of solutions we need to closely look at the autonomous equation.

There are four interesting lines on which the denominator or the numerator is equal to zero or equivalently, $dv/du = 0$ or $du/dv = 0$. Characteristic features of those four lines are plotted in Figs. 1 and 2.

We call the thick-red lines R1 and R2 on which only u changes its value ($dv/du = 0$) and C crosses the lines horizontally:

$$\text{R1: } v = 0, \quad \text{R2: } v - v_T = s(u - 1). \quad (3.1)$$

Energy density $\rho \sim v$ is zero on the line R1. Because R1 is horizontal, solution curves are allowed to touch R1 only at a special points $\mathcal{O}(0, 0)$ and $\text{P}_E(1, 0)$.

We call the thick-black lines B1 and B2 on which only v changes its value ($du/dv = 0$) and C crosses the lines vertically:

$$\text{B1: } u = 1, \quad \text{B2: } u = 2v. \quad (3.2)$$

⁵ One can confirm that all three solutions in Ref. [1] satisfy this relation. For the case that w_1 depends on r , $w_1 = w_1(r)$ as in Ref. [23], one can show that $m'(r_T) = -1/2w_1(r_T)$.

The line B1 represents a static boundary where g_{rr} changes its signature. Because the line B1 is parallel to the v axis, C is allowed to cross the line only through P_E , where the subscript E represents event horizon. Since we focus on static traversable wormhole solutions in this work, we restrict our interests to the region with $u \leq 1$. As will be shown later in this work, a solution having a wormhole ‘throat’ does not have an event horizon, i.e., its solution curve never crosses B1. Note that solution curves never become vertical or horizontal at the points which are not on the lines R1, R2, B1, and B2.

The crossing points between the black lines and the red lines are

$$\mathcal{O}(0,0), \quad P_E(1,0), \quad P_T(1,v_T), \quad P_B(2v_B,v_B), \quad (3.3)$$

where $v_B \equiv 2w_2/[(1+w_1)^2 + 4w_2]$. \mathcal{O} plays the role of an asymptotic geometry of $r \rightarrow \infty$ for the wormhole spacetime. The point P_T is a wormhole ‘throat’. The point P_B represents a point where all solution curves bounce back.

The radial dependence of a solution curve C on the (u, v) plane can be obtained from

$$\frac{dr}{r} = \frac{du}{2v-u} = \frac{-1}{1+w_1} \frac{1-u}{v[v-v_T+s(1-u)]} dv, \quad (3.4)$$

where the second equality comes from Eq. (2.10). The relation can be interpreted as:

- The radius increases/decreases with u when the curve is above/below the line B2, respectively.
- The radius increases or decreases with v depending on many factors. They are the signature of $1+w_1$ and whether the curve is above or below the lines R1 and R2.

Hence, the region $(u < 1, v)$ is divided into 7 regions maximally by the 3 lines, R1, R2 and B2. The increasing direction of r varies region by region. The ‘cyan’ arrows in the figures in this work denote the increasing direction of r . One can intuitively notice how the solution (mass and density) develops as one moves from the ‘throat’ to the outside regions.

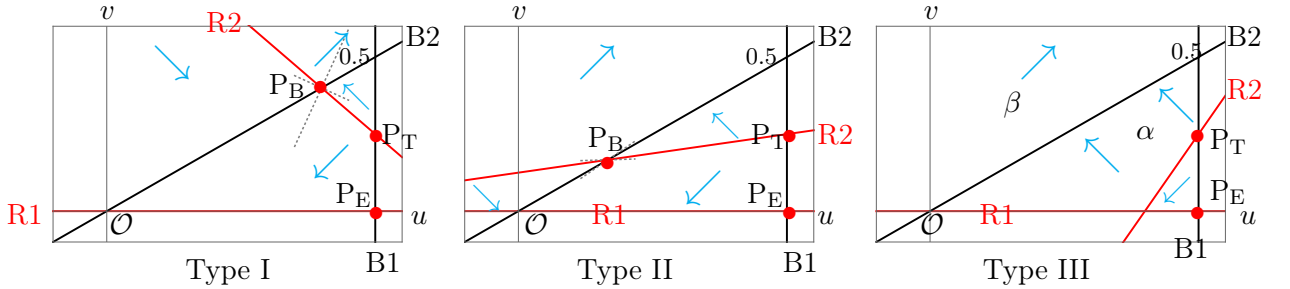


Figure 1. Classification of the autonomous equation for $w_1 < -1$. The cyan arrows represent the increasing direction of radial coordinate r . The direction changes based on the lines B2 and R2. The red line R2 changes depending on the values of w_i .

As an example, let us apply the above properties to the Type I and II of the Fig. 1. Consider a solution curve which passes P_T vertically. If it goes vertically upwards from P_T the solution curve C bends to the left following the arrow until the curve meets the line B2 or R2. If it touches the line B2, the curve bends upwards and approaches the line B1 indefinitely. This asymptotic behavior with $v = m'(r) \rightarrow \infty$ can be excluded as a physically viable regular solution. By applying same consideration, one can figure out genuine solutions and double check if the solutions follow the arrows.

3.1 Analysis for $w_1 < -1$

Let us first consider the case with $w_1 < -1$. In this case, $v_T > 0$. By means of the slope s of the line R2, we divide the deployment of the points and the lines into three different types as in Fig. 1,

$$\text{I: } s < 0 \left(w_2 > -\frac{1+w_1}{4} \right), \quad \text{II: } 0 \leq s \leq v_T \left(0 \leq w_2 \leq -\frac{1+w_1}{4} \right), \quad \text{III: } s > v_T \ (w_2 < 0).$$

For the Types I and II the point P_B is in the region we are interested in ($0 \leq u < 1$). For the Type III, P_B is located outside of the physical region. In Sec. 5, we display exact solutions which belong to the types I and II.

Even though there is a wormhole throat, the solutions in the Type III does not have a regular asymptotic region: Most of the solution curves allowing a wormhole ‘throat’ pass the point P_T with $u \leq 1$ and tangent to the line B1 at the ‘throat’ except a symmetric solution described in Sec. 3.3.2. Let us consider one of the curves. A solution curve may depart from P_T vertically upwards (increasing v , decreasing u) and downwards (decreasing u and v). As one can see clearly from the arrows, the first one that starts from the region α continues until it meets the line B2 and becomes vertical followed by entering the region β . Once a solution curve enters the region β it goes upwards to a singular region $v \rightarrow \infty$ until the curve becomes parallel to the line B1 ($u = 1$). The second one touches R2 at some point⁶, and becomes horizontal there entering to the region α . In this region, v cannot decrease but only increases until C meets the line B2. There, C becomes vertical again and enters the region β and repeats the same behavior as above. In summary, both ends of C give infinity value of v , implying singularities. Therefore, later in this work, we consider only the type I and II with $w_2 \geq 0$.

3.2 Analysis for $w_1 > 0$

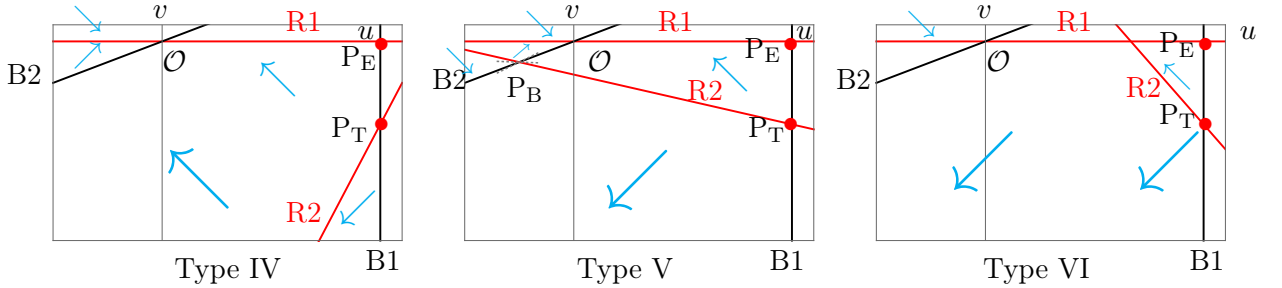


Figure 2. Classification of the autonomous equation for $w_1 > 0$. The direction changes based on the line B2, R1 and R2.

In this case, since $v_T < 0$, the energy density near the wormhole ‘throat’ is negative. There are three types:

$$\text{IV: } s > 0 \left(w_2 < -\frac{1+w_1}{4} \right), \quad \text{V: } v_T \leq s \leq 0 \left(-\frac{1+w_1}{4} \leq w_2 \leq 0 \right), \quad \text{VI: } s < v_T \ (w_2 \geq 0).$$

⁶ If the curve C touches R1, it is possible only at P_E in principle. This is not possible because the autonomous equation implies that the solution is analytic. Putting the trial function $u = 1 - \kappa|v|^\beta$ with $\kappa|v|^\beta \ll 1$ to Eq. (2.10) we get $\beta = (-2w_1)/(1+w_1) < 0$. Therefore, the solution curve C never meet the point P_E but bounces for any value of $\kappa \neq 0$. This implies that event horizons will never be formed.

We first show that the Type VI does not allow a regular wormhole solution as in the Type III for $w_1 < -1$. Let us consider a solution curve C passing P_T vertically. Vertically upward part of the curve becomes horizontal when it meets the red lines R1 or R2. As can be understood in the figure, the curve will cross R2 before it meets \mathcal{O} and becomes parallel to the u axis. Then, by similar consideration above (when $w_1 < -1$), the solution curve after crossing the line R2 goes to the region $(u, v) \rightarrow (-\infty, -\infty)$. Vertically downward part of the curve at P_T cannot be a parallel to the $v = 0$ line because it never meet a red line. Again, the curve goes to the region $(u, v) \rightarrow (-\infty, -\infty)$. In this case, a space-time singularity will form there.

On the other hand, for the type IV, the vertically upward part of C can approach \mathcal{O} , hence some solutions follow the path. The vertically downward part of C can meet R2 and becomes parallel and the value v starts to increase. In that case, some curve can also approach the point \mathcal{O} . Therefore, there are possibilities that both ends of a solution curve finish at \mathcal{O} , forming regular asymptotic regions. Similar analysis for the type V leads that only upward curves have a possibility to approach \mathcal{O} , to form a regular solution.

To summarize, we are mainly interested in the cases with Type I, II, IV, and V. For all the cases, $w_1 w_2 < 0$ is satisfied. Therefore, isotropic fluid fails to form a regular wormhole spacetime.

3.3 behaviors around important points

To have clear pictures, we study properties of solutions around a few important points. One of them is \mathcal{O} which represents asymptotic limit ($r \rightarrow \infty$) for the types I, II, IV and V. Other important points are P_T and P_B , representing a wormhole ‘throat’ and the bouncing point, respectively.

3.3.1 The asymptotic behavior around \mathcal{O}

Let us first search for the behavior of C around the point $\mathcal{O}(0, 0)$. Because $|u|, |v| \ll 1$ around \mathcal{O} , Eq. (2.10) can be approximated as

$$u'(v) = \alpha \left(\frac{u}{v} - 2 \right), \quad \alpha = -\frac{w_1}{2w_2}. \quad (3.5)$$

Solving the equation gives

$$u = \begin{cases} \frac{2\alpha}{\alpha-1}v + qv^\alpha & (\alpha \neq 1), \\ -2v \log |v| + q'v & (\alpha = 1), \end{cases} \quad (3.6)$$

where q and q' are integration constants. Because we are interested only in $w_1 w_2 < 0$ case, the constant α takes positive value ($\alpha > 0$)⁷. The solution curve of a regular wormhole should not end in the region $u \rightarrow -\infty$ or $v \rightarrow \infty$. Thus, both ends of a solution curve should be located at \mathcal{O} . In this sense, the point \mathcal{O} plays the role of an asymptotic infinity.

In Eq. (3.6), when $\alpha > 1$, the linear behavior dominates since $v^\alpha \ll 1$. When $0 < \alpha < 1$, the power law behavior (the v^α term) dominates. When $\alpha = 1$, the solution takes $u \sim -2v \log |v|$ behavior.

⁷It is to be noted that when $\alpha < 0$, Eq. (3.6) implies that the solution curve never passes the point \mathcal{O} unless $q = 0$. Therefore, only linear behavior exists at \mathcal{O} .

For $w_1 < -1$ and $-2w_2 = 1 + w_1$, we have $\alpha = 1 + 1/2w_2 > 1$ since $w_2 > 0$. This means the linear behavior is favored. We present an exact solution later in Eq. (5.1). On the other hand, when $0 < w_1 < -2w_2$, the power law behavior is favored for $q \neq 0$ and the exact solution (5.1) is not a favorable behavior around the origin.

The radius can be expressed in terms of v as

$$r = r_0 v^{-\alpha},$$

where r_0 is a constant. The mass function at r becomes

$$m(r) = \frac{ur}{2} = \frac{r_0}{2} \left[q - \frac{2\alpha}{1-\alpha} \left(\frac{r}{r_0} \right)^{(\alpha-1)/\alpha} \right]. \quad (3.7)$$

This mass function approaches a finite value $qr_0/2$ asymptotically only when $0 < \alpha < 1$ ($-2w_2 < w_1 < 0$ or $0 < w_1 < -2w_2$). When $\alpha \geq 1$ ($0 < w_2 \leq -w_1/2$), the mass function diverges.

The g_{tt} part of the metric is constant around \mathcal{O} ,

$$f(r) = f_0 \left(\frac{r}{r_0} \right)^{\frac{4w_2}{1+w_1}} \left(\frac{v}{v_0} \right)^{-\frac{2w_1}{1+w_1}} \approx f_0 (v_0)^{\frac{2w_1}{1+w_1}} = \text{constant},$$

where we use Eq. (2.8) with the relation $v = 4\pi r^2 \rho$. The density becomes

$$\rho = \frac{v}{4\pi r^2} = \frac{1}{4\pi r_0^2} \left(\frac{r_0}{r} \right)^{2-2w_2/w_1}.$$

3.3.2 Behavior of around a wormhole ‘throat’ P_T

Let us search for the behavior of a solution curve C around the ‘throat’ $P_T(1, v_T)$. By using the trial function $1 - u = \kappa|v - v_T|^\beta$ around $u \sim 1$, we find that Eq. (2.10) allows a quadratic and a linear behaviors for C ,

$$\text{i) The asymmetric solution } \quad \beta = 2, \quad u = 1 - \kappa(v - v_T)^2, \quad (3.8)$$

$$\text{ii) The symmetric solution } \quad \beta = 1, \quad u = 1 - s^{-1}(v - v_T), \quad (3.9)$$

where κ represents an arbitrary real number and s is given in Eq. (2.12). Here ‘asymmetric’/‘symmetric’ implies that the geometric structure is asymmetric/symmetric with respect to the inversion relative to the throat, respectively.

For the case i), the radius takes the form,

$$r \approx r_T \left[1 + \frac{w_1 \kappa}{1 + w_1} (v - v_T)^2 \right]. \quad (3.10)$$

Therefore, r takes minimum value at $v = v_T$ when $\kappa > 0$. As will be shown in the numerical plot, the symmetric solution appears as a large κ limit of the asymmetric solution. The example of the exact time-symmetric solution will be given in Eq. (5.1) when $1 + w_1 + 2w_2 = 0$ i.e. $s = -v_T$.

It appears that u, v and du/dv are continuous at P_T for solution curves with different κ . Therefore one should check whether solutions with different κ can be attached smoothly to form a proper wormhole solution or not. To answer this question, let us calculate the extrinsic curvatures for both cases. As in Ref. [18] we divide a wormhole spacetime into two

regions and denote Σ_+, Σ_- as the hypersurfaces at $r = r_T$ in each side of the throat. Then in our coordinate, the extrinsic curvatures are

$$K_{ab}^\pm = \frac{1}{2} \frac{\partial g_{ab}^\pm}{\partial r}, \quad a = t, \theta, \phi. \quad (3.11)$$

Since $K_{\theta\theta}, K_{\phi\phi}$ have the same values on both sides, we consider K_{tt} only here. From the metric Eq. (2.3) and the form of g_{tt} in Eq. (2.8), we have

$$K_{tt} = -\frac{1}{2} \frac{df}{dr} = \left(-\frac{2w_2}{1+w_1} \frac{1}{r} + \frac{w_1}{1+w_1} \frac{1}{v} \frac{dv}{dr} \right) f(r). \quad (3.12)$$

By using Eq. (3.4) and the above relations (3.8),(3.9), the K_{tt} behaves as

$$K_{tt} = \begin{cases} \left(\frac{1}{2} - \frac{w_1}{\kappa(v-v_T)} \right) \frac{f(r_T)}{r_T}, & \beta = 2, \\ \left(1 + \frac{2w_2}{1+w_1} \right) \frac{f(r_T)}{r_T}, & \beta = 1. \end{cases} \quad (3.13)$$

Thus for $\beta = 1$ case, two solutions can be attached smoothly. However, for $\beta = 2$ case, the boundaries form a ‘surface layer’ where $K_{ab}^+ \neq K_{ab}^-$, they cannot be attached without a junction condition unless they have same κ .

3.3.3 behavior around the bouncing point P_B

Let us approximate the differential equations (2.10) and (3.4) around P_B . After setting $u = u_B + x$ and $v = v_B + y$, they can be written as, to the linear order in x and y ,

$$\frac{d}{d \log r} \begin{pmatrix} x \\ y \end{pmatrix} = \begin{pmatrix} -1 & 2 \\ (1-\gamma)s & \gamma-1 \end{pmatrix} \begin{pmatrix} x \\ y \end{pmatrix}, \quad \gamma \equiv 1 - \frac{2w_2}{1+w_1} = \frac{3}{2} + w_1 s > 0. \quad (3.14)$$

Defining new variables $X_\pm = y - \frac{\gamma \pm \sqrt{\gamma^2 + 8s(1-\gamma)}}{2s(1-\gamma)} x$, Eq. (3.14) is reduced to a diagonal form,

$$\frac{dX_\pm}{d \log r} = \epsilon_\pm X_\pm; \quad \epsilon_\pm = \frac{-2 + \gamma \mp \sqrt{\gamma^2 + 8s(1-\gamma)}}{2}. \quad (3.15)$$

Note that the term in the square-root is

$$D \equiv \gamma^2 + 8s(1-\gamma) = w_1(w_1 - 8)(s - s_+)(s - s_-), \quad (3.16)$$

where

$$s_\pm = \frac{4 - 3w_1 \pm 4\sqrt{1 + 3w_1}}{2w_1(w_1 - 8)}. \quad (3.17)$$

If $D < 0$, the eigenvalues ϵ_\pm have imaginary parts and the solution curve C has a spiral behaviors asymptotically as depicted in Ref. [24]. In our case, this never happens. The proof is the following:

- $w_1 < -1$

Interpreting D as a quadratic function of real number s , one can find that $D = 0$ does not have a real valued solution. In other words, s_\pm are imaginary. Hence D is always positive because $w_1(w_1 - 8) > 0$. Therefore, when $w_1 < -1$, one never gets a ‘spiral’ solution.

- $w_1 > 0$. In this case, s_{\pm} are real numbers.
 1. $0 < w_1 < 8$, ($s_+ < s_-$): In order for $D > 0$, s should satisfy $s_+ < s < s_-$. As seen in Fig. 2, the point P_B is in a physical region only for the type V, which restricts $v_T \leq s \leq 0$. At the present case, $s_+ < v_T$ and $s_- > 0$. Therefore, D is positive definite.
 2. $w_1 = 8$: In this case, $D = 0$ and the eigenvalues are real-valued with $\epsilon_+ = \epsilon_-$.
 3. $w_1 > 8$, ($s_- < s_+$): In order for $D > 0$, $s < s_-$ or $s > s_+$. Since physical region of s is $(v_T, 0)$, in order to avoid the ‘spiral’ curve, $(s_-, s_+) \cap (v_T, 0)$ needs to be an empty set. One can show that $s_+ < v_T$ for $w_1 > 8$. Consequently, the ‘spiral’ curve never happens.

Since we always have $D > 0$, the curve C in the (X_+, X_-) coordinates satisfies

$$X_{\pm} = X_{\pm,0} \left(\frac{r}{r_B} \right)^{\epsilon_{\pm}} \rightarrow \frac{X_-}{X_+} = \frac{X_{-,0}}{X_{+,0}} r^{-\sqrt{D}}, \quad (3.18)$$

where $X_{\pm,0}$ is an integration constant. In other words, as r increases towards r_B , the curve changes gradually (not oscillating) to the limit $(X_{-,0}/X_{+,0}) r_B^{-\sqrt{D}}$.

This gives $X_-/X_+ = (X_-/X_{-,0})^{\epsilon_+/\epsilon_-}$. For types I, II and V, where ϵ_{\pm} are real,

$$\epsilon_+ \epsilon_- = \frac{2w_2}{w_1} \left(1 + \frac{4w_2}{(1+w_1)^2} \right) < 0.$$

This implies that every solution curve follows in along one of the X_{\pm} and follows out the other axis without touching the point P_B . Note that for the type IV, the bouncing point is located outside of the region we are interested in.

4 Numerical solutions

In this section, we display numerical solutions of the Einstein’s equation (2.10) on the (u, v) plane to show behaviors of solutions.

4.1 $w_1 < -1$ case

A regular wormhole solution made of an anisotropic matter with non-negative energy density exists only for the Type I, where $w_1 < -1$ and $w_2 > -(1+w_1)/4$. A well-localized solution having finite total mass exists when $w_2 > -w_1/2$. Therefore, we restrict our interests only to this situation.

1. *Symmetric Solution*: The blue curve in Fig. 3 corresponds to the linear behavior ii) at P_T in Eq. (3.9). The curve represents half of the wormhole solution from the ‘throat’ at P_T to an asymptotic region at \mathcal{O} . The other half of the wormhole can be added by duplicating the curve.
2. *Asymmetric Solution*: The gray curve presents a solution curve corresponding to a regular wormhole. In this case, the geometry of the wormhole is not symmetric with respect to the ‘throat’. Any curve which begins at P_T and ends at \mathcal{O} represents half of the spacetime including a ‘throat’ and an asymptotic region. In the lower part of the gray curve, the value of u monotonically decreases and forms an asymptotically flat

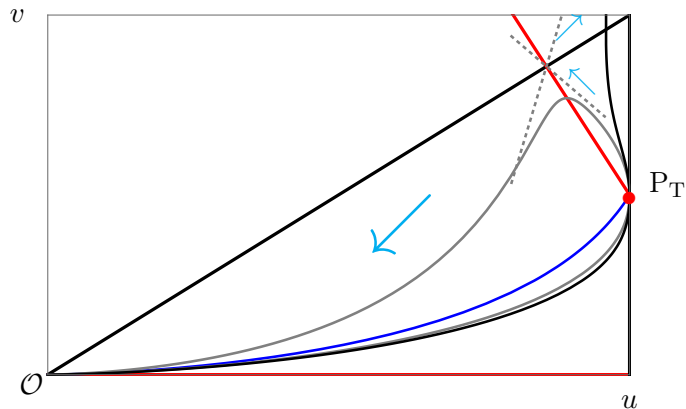


Figure 3. Numerical solutions for the Type I with $w_1 = -2$ and $w_2 = 1.5$.

region at \mathcal{O} . While, for the case of the solution curve corresponding to the other half, u bounces back around P_B and decreased. Then, it also forms the other asymptotically flat region at \mathcal{O} .

3. *Solution with one asymptotic region:* Two ends of the black curve go into the region \mathcal{O} and $v \rightarrow \infty$, respectively. The wormhole ‘throat’ is located at P_T . Following the upper part of the black curve, the radius increases to a finite value as $v \rightarrow \infty$. Therefore, a singularity of density exists.

4.2 $w_1 > 0$ case

In this case, the energy density is negative definite. A regular wormhole solution exists only for the Type IV, where $w_2 < -(1 + w_1)/4$. A well localized solution having finite total mass exists when $0 < w_1 < -2w_2$. Therefore, we restrict our interests only to this situation.

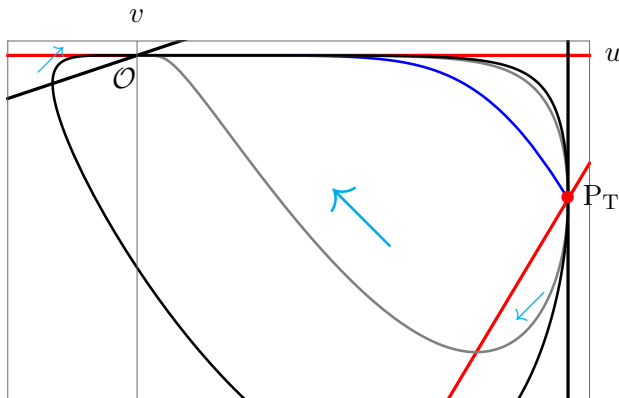


Figure 4. Numerical solutions for the type IV with $w_1 = 2$ and $w_2 = -3$.

1. *Symmetric Solution:* The blue curve in Fig. 4 corresponds to the linear behavior ii) at P_T in Eq. (3.9). The curve represents half of the wormhole solution from the ‘throat’ at P_T to an asymptotic region at \mathcal{O} . The other half of the wormhole can be added by duplicating the curve.

2. *Asymmetric Solution I:* The gray curve presents a solution curve corresponding a regular wormhole in which the mass takes positive values in all the spacetime. In this case, the geometry is not symmetrical around the ‘throat’.

In the upper part of the gray curve, the value of u monotonically increases and forms an asymptotically flat region at \mathcal{O} . While, for the case of the solution curve corresponding to the other half, u decreases at the beginning but bounces back to increase. Then, it also forms the other asymptotically flat region at \mathcal{O} .

3. *Asymmetric solution II:* Two ends of the black curve go into the point \mathcal{O} . In this case, one end of C approach \mathcal{O} from the negative value of u . Therefore, the mass function becomes negative in this region. Only the asymptotic behaviors around the point \mathcal{O} is different from the first case.

5 Exactly solvable cases

Even though one cannot find a general solution of Eq. (2.9) it is still possible to find a few new specific solutions. In this section, we present two exact solutions for the cases $w_2 = -(1 + w_1)/2$ and $w_2 = -(1 + w_1)/4$.

5.1 Specific solution for the case $1 + w_1 + 2w_2 = 0$

First, we present a specific solution for the matter which is marginal to the strong energy condition $\rho + \sum_i p_i \geq 0$. That is, when $\rho + \sum_i p_i = (1 + w_1 + 2w_2)\rho = 0$, Eq. (2.9) permits a solution. In this case, the slope $s = 1/2w_1 = -v_T$.

Now, one can readily check that Eq. (2.10) allows a linear solution curve

$$v = v_T u. \quad (5.1)$$

In fact, one of the solution found in Ref. [1] is a special case of this when $w_1 = -2$. This linear solution plays an important role in analyzing the solution space of Eq. (2.10).

The radius and density behaves as

$$r = r_T \left(\frac{v}{v_T} \right)^{-w_1/(1+w_1)}, \quad \rho = \frac{v}{4\pi r^2} = \frac{v_T}{4\pi r_T^2} \left(\frac{r_T}{r} \right)^{3+1/w_1}. \quad (5.2)$$

At the point $\mathcal{O}(0,0)$, the radius diverges to form a regular asymptotic region. At the point $r = r_T$, it forms a wormhole ‘throat’ at $v = v_T$. The mass function becomes

$$m(r) = \frac{ru}{2} = \frac{r_T}{2} \left(\frac{r}{r_T} \right)^{-\frac{1}{w_1}}.$$

Therefore, as $r \rightarrow \infty$, the total mass inside r becomes divergent/zero when $w_1 \leq 0$. The metric function $f(r) = f_0$ is independent of r . The metric function $g_{rr} = [1 - (r_T/r)^{(1+w_1)/w_1}]^{-1}$ linearly diverges as $r \rightarrow r_T$, which is a signature of the wormhole ‘throat’. For $w_1 > 0$, the mass monotonically decreases from $r_T/2$ to zero as $r \rightarrow \infty$.

5.2 Various solutions for case $1 + w_1 + 4w_2 = 0$

A new wormhole solution exists in this case. The strong energy condition will be violated for $w_1 < -1$ because $1 + w_1 + 2w_2 = -2w_2 < 0$. Since the slope $s = 0$, the denominator of Eq. (2.10) has no u dependence and the equation is integrable exactly to give

$$u = 1 - \frac{\left(1 - \frac{v}{v_T}\right)^2}{1 + \frac{2w_1}{1-w_1} \left(\frac{v}{v_T}\right) - c_1 \frac{1+w_1}{1-w_1} \left(\frac{v}{v_T}\right)^{\frac{2w_1}{1+w_1}}}. \quad (5.3)$$

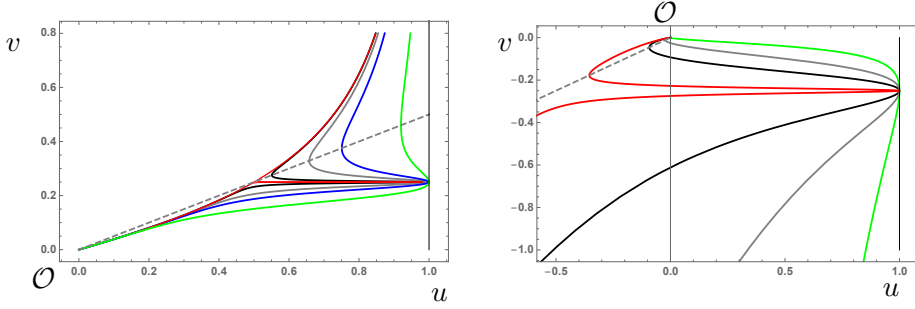


Figure 5. Various solution curves with $c_1 > 1$ for $(w_1, w_2) = (-2, 1/4)$ (Left) and $(2, -3/4)$ (Right). Here $c_1 = 1.001, 1.1, 1.5, 2$, and 4 , respectively for red, black, gray, blue, and green curves. Every solution curves with $c_1 > 1$ pass the point $(u, v) = (1, v_T)$ where a wormhole ‘throat’ forms.

The characteristic behaviors of the solution curves with $c_1 > 1$ are given in Fig. 5 in which $w_1 = 2$ and -2 , respectively for the left and the right panels. We neglected the curves with $c_1 \leq 1$ because they do not contain a wormhole ‘throat’. For both the cases, one end of the solution curves finishes at \mathcal{O} , which corresponds to an asymptotic infinity at $r \rightarrow \infty$. The other end finishes at $v \rightarrow \infty$ or $(u, v) \rightarrow (-\infty, -\infty)$, respectively for $w_1 < -1$ or $w_1 > 0$, where a singularity forms.

Let us observe the behaviors of the solutions in detail. Around $v = v_T$, it becomes, for $c_1 \geq 1$,

$$u \approx 1 + \frac{4w_1^2}{(c_1 - 1)} \frac{1 - w_1}{1 + w_1} (v - v_T)^2, \quad c_1 > 1; \quad u \approx -\frac{1}{w_1} - \frac{2(v/v_T - 1)}{3w_1}, \quad c_1 = 1.$$

Therefore, Eq. (5.3) presents a relevant wormhole ‘throat’ when $c_1 > 1$ because $u \leq 1$ in this case. On the other hand, when $c_1 = 1$, the curve does not pass the point $(u, v) = (1, v_T)$, the ‘throat’. Incidentally, the value of κ in Eq. (3.8) is related with c_1 by

$$\kappa = \frac{4w_1^2}{1 - c_1} \frac{1 - w_1}{1 + w_1}.$$

Around \mathcal{O} , the asymptotic region, u behaves as

$$u \approx \begin{cases} \frac{2}{1-w_1} \frac{v}{v_T}, & |w_1| > 1, \\ -c_1 \frac{1+w_1}{1-w_1} \left(\frac{v}{v_T}\right)^{\frac{2w_1}{1+w_1}}, & 0 < w_1 < 1, \\ \frac{v}{v_T} \log \frac{c_1 v}{v_T}, & w_1 = 1. \end{cases} \quad (5.4)$$

When $|w_1| > 1$, the linear behavior dominates. On the other hand, when $0 < w_1 < 1$, polynomial behavior dominates.

The radius can be obtained by using Eqs. (2.10) and (3.4):

$$r = r_T \left(\frac{v}{v_T} \right)^{-\frac{2w_1}{1+w_1}} \frac{1-w_1}{(1+w_1)(1-c_1)} \left(1 + \frac{2w_1}{1-w_1} \frac{v}{v_T} - c_1 \frac{1+w_1}{1-w_1} \left(\frac{v}{v_T} \right)^{\frac{2w_1}{1+w_1}} \right). \quad (5.5)$$

The radius takes its minimum value r_T at the ‘throat’ $v = v_T$. As v decreases, the radius goes to infinity at $v = 0$. On the other hand, as $v \rightarrow \infty$ it increases to a local maximum value $r_T/(c_1 - 1)$ or goes to infinity as $r \rightarrow r_+/(1 - c_1) \times (2w_1/(1 + w_1))(v/v_T)^{(1-w_1)/(1+w_1)}$, respectively for $|w_1| > 1$ or $0 < w_1 < 1$.

The mass function behaves as

$$m = \frac{ur}{2} = \frac{r_T}{(1-c_1)(1+w_1)} \left(\frac{v}{v_T} \right)^{\frac{1-w_1}{1+w_1}} \left[1 - \frac{1-w_1}{2} \frac{v}{v_T} - c_1 \frac{(1+w_1)}{2} \left(\frac{v}{v_T} \right)^{-\frac{1-w_1}{1+w_1}} \right]. \quad (5.6)$$

For $w_1 < -1$, the mass function has a divergent value for large r ($v \rightarrow 0$). This is a signature of the instability of the wormhole ‘throat’. The mass decreases to $m(v_T) = r_T/2$ and then bounces back to increase to a finite value $m(v \rightarrow \infty) = r_T c_1/2(c_1 - 1)$. For $w_1 > 1$, the mass diverges at $v \rightarrow 0$. On the other hand, for $0 < w_1 < 1$, it goes to a constant value $m(v = 0) = r_T c_1/2(c_1 - 1)$.

The g_{tt} part of the metric function from Eq. (2.8) becomes

$$f(r) = f_0 \left(\frac{r}{r_0} \right)^{\frac{4(w_2-w_1)}{1+w_1}} \left(\frac{\rho}{\rho_0} \right)^{-\frac{2w_1}{1+w_1}} = f_0 \left(\frac{r}{r_0} \right)^{\frac{4w_2}{1+w_1}} \left(\frac{v}{v_0} \right)^{-\frac{2w_1}{1+w_1}}. \quad (5.7)$$

One may also check the two formula for $f(r)$ in Eqs. (2.7) and (2.8) present the same result.

Although the two exact solutions discussed in this section have deficits of their own, they provide good insights on the general solution space.

6 Special Solutions

6.1 Perturbative solution for $1 + w_1 + 2w_2 = 0$ case

Around the exact solution $v = v_T u$ when $s = -v_T = 1/2w_1$, we can find a nearby solution by setting

$$v = -\frac{u}{2w_1} + \delta v(u),$$

Equation (2.10) becomes

$$\frac{d}{du} \delta v = \left[\frac{w_1}{(1+w_1)u} - \frac{1}{2(1-u)} \right] \delta v.$$

Solving this equation gives

$$v = -\frac{u}{2w_1} + \delta v = -\frac{u}{2w_1} + \delta v_0 \cdot (1-u)^{1/2} u^{w_1/(1+w_1)}, \quad \delta v_0 \ll 1. \quad (6.1)$$

For $w_1 < -1$, the solution is valid over all the region with $0 \leq u \leq 1$. On the other hand, when $w_1 > 0$, the solution may not valid around $u \lesssim |\delta v_0/v_T|^{1+w_1}$. In this case the solution around $u \sim 0$ is given in Eq. (3.6),

$$\frac{u}{v} = -2w_1 \left[1 + q(-2w_1 v)^{-1/(1+w_1)} \right] \quad |v| \ll |v_T|, \quad (6.2)$$

The two solutions should be matched in the region $|2w_1 \delta v_0|^{1+w_1} \ll u \ll 1$. Matching v/u gives,

$$\frac{-2w_1 v}{u} \approx \left(\frac{q}{2w_1 \delta v_0} \right)^{1+w_1} \Rightarrow q = 2w_1 \delta v_0,$$

because $v/u \approx -1/2w_1$ in this region. The radial coordinate relation (3.4) becomes

$$\frac{dr}{r} = \frac{du}{2v-u} \approx -\frac{w_1}{1+w_1} \frac{du}{u} - \frac{w_1^2 \delta v}{(1+w_1)^2} \frac{du}{u^2},$$

where $\delta v_0 \ll 1$ is assumed in the second equality. This gives

$$\log \frac{r}{r_T} = \frac{1}{2v_T-1} \log u + \frac{2\delta v_0}{3(2v_T-1)^2} (1-u)^{3/2} {}_2F_1 \left(\frac{3}{2}, \frac{w_1+2}{w_1+1}, \frac{5}{2}, 1-u \right).$$

6.2 Limiting solution for $|s| \gg 1$

One can rewrite the TOV equation (2.10) as

$$\frac{du}{dv} = \frac{-1}{1+w_1} \left(\frac{2v-u}{v} \right) \frac{1-u}{v-su-v_s}, \quad v_s \equiv v_T - s = \frac{2w_2}{w_1(1+w_1)} \quad (6.3)$$

One can see that when the value of s is large, the value of v_s is also large. One can rewrite v_s as

$$v_s \equiv -as, \quad a \equiv \frac{4w_2}{1+w_1+4w_2}. \quad (6.4)$$

Now, the TOV equation can be rewritten as a series of s^{-1}

$$\begin{aligned} \frac{du}{dv} &= \frac{-1}{1+w_1} \frac{(2v-u)(1-u)}{v[v-s(u-a)]} \\ &= -\alpha \left(\frac{2v-u}{v} \cdot \frac{1-u}{1-u/a} \right) \left[1 + \frac{v}{a-u} s^{-1} + \dots \right], \end{aligned} \quad (6.5)$$

where $\alpha = 1/(1+w_1)as = -w_1/2w_2$ was defined in Eq. (3.6). The general behavior of the 0th order solution is the same as that of the solution around \mathcal{O} given in Eq. (3.6).

$$u = -\frac{2\alpha}{1-\alpha} v + qv^\alpha, \quad (6.6)$$

where q is an integral constant. For a solution curve to pass the point \mathcal{O} , we should take $\alpha > 0$ because $v^\alpha \rightarrow \infty$ when $\alpha < 0$. Note that when α is given, the trajectories are classified by q only.

In Fig. 6, characteristic picture of the limiting solution is given. The blue curve represents a regular wormhole solution which is symmetric with respect to the ‘throat’. As seen in the figure, the curve gradually decreases to \mathcal{O} with r .

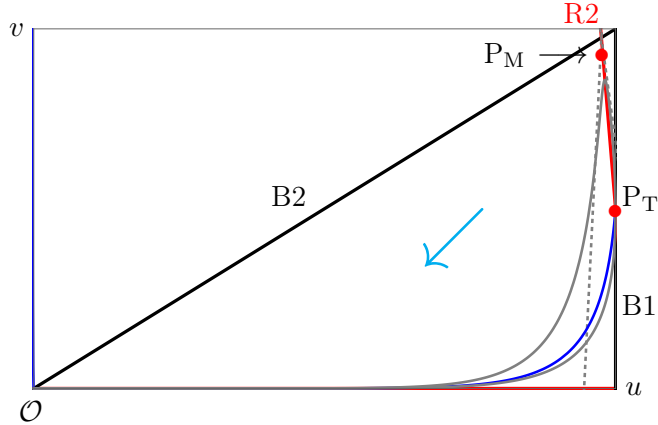


Figure 6. Characteristic picture of limiting solution of Type I with $w_1 < -1$.

The gray curve in Fig. 6 represents an asymmetric wormhole solution which is regular over the whole spacetime when $w_1 < -1$. Considering the upper half of the curve starting from the point P_T , the value of v increases to a maximum value at P_M and then decreases to zero as one approaches the asymptotic region. Let the coordinates of P_M be (u_m, v_m) . Then we have

$$\left. \frac{dv}{du} \right|_m = 0, \quad v_m = s(u_m - a), \quad a \equiv \frac{4w_2}{1 + w_1 + 4w_2}. \quad (6.7)$$

Let us introduce a new coordinates (x, y) around P_M as $u \equiv u_m + x, v \equiv v_m + y$. Then Eq. (2.10) can be approximated for small $|x|, |y| \ll 1$ and $|y| \ll |sx|$ to be

$$\frac{dy}{dx} = -c_m \left[x + \left(\frac{1}{1 - u_m} + \frac{1}{2v_m - u_m} \right) x^2 + \dots \right] \Rightarrow y = -\frac{1}{2}c_m x^2 + \mathcal{O}(x^3), \quad (6.8)$$

where

$$c_m = \left| \frac{(1 + w_1)sv_m}{(1 - u_m)(2v_m - u_m)} \right| = \left| \frac{a}{\alpha} \frac{v_m}{(1 - u_m)(2v_m - u_m)} \right|. \quad (6.9)$$

The solution curve has approximately quadratic form around P_M , $y = -\frac{1}{2}c_m x^2$. As one moves farther from the maximum point, the curve takes higher order functions of x .

When $|s|$ becomes large, the line R2 approaches the line B1 and $a \rightarrow 1, 1 - u_m \rightarrow 0$. For the asymmetric solution, the maximum point P_M goes near the bouncing point P_B ($2v_m - u_m \rightarrow 0$). That is, $c_m \rightarrow \infty$. This means the solution curve becomes very steep and narrow as $|s| \rightarrow \infty$ as shown in Fig. 6. Hence, in the limit, the derivative of an asymmetric curve is discontinuous at P_M . As $u_m \rightarrow 1$, the curve mostly can be divided into the left part and the right part of P_M .

Solution curves around \mathcal{O} are under the line B2 ($v < u/2$). Thus to meet P_M or P_T , derivative of the solution takes only positive value:

$$\frac{dv}{du} = \frac{1}{\frac{2\alpha}{\alpha-1} + \alpha q v^\alpha} = \frac{v}{\alpha(u - 2v)} > 0, \quad (6.10)$$

for positive v . Therefore the type of solution (6.6) either can be extended to meet symmetric solutions (to P_T) or to meet the left part of the asymmetric solutions (to P_M) depending on the values of α and q .

7 Summary and Discussions

We have classified static spherically symmetric wormhole solutions consist of an anisotropic matter throughout the entire spacetime and studied necessary conditions for nonsingular wormholes to exist. In the process, we found a few exact solutions in special configurations. We also presented wide variety of solutions by studying the properties they generally have. The behavior of wormhole geometry and physical quantities around important points such as the ‘throat’, the bouncing point and the asymptotes have been studied. Numerical solutions have also been presented to give insights about the behaviors of general solutions.

An anisotropic matter of the limit $w_1 \equiv p_1/\rho \rightarrow -1$, resembles the stress tensor of radial electric field which may be used to produce a charged wormhole in Ref. [3]. This corresponds to the $|s| \rightarrow \infty$ limit which we analyzed in Sec. 6.2. From the asymptotic form of the solution in Eq. (6.6), the part of the solution near maximum v in Eq. (6.8) and the numerical solution, one can figure out how the solution behaves. However, we observed that there is no wormhole solution when $w_1 = -1$. One may ask the case that corresponds to a charged wormhole solution, for example, that in Ref. [3]. There, the energy density and the pressure are given by

$$\begin{aligned}\rho &= \rho^{(0)} + \rho^{(1)}, \\ p_1 &= p_1^{(0)} + p_1^{(1)},\end{aligned}\tag{7.1}$$

where $(\rho^{(0)}, p_1^{(0)})$ are those of non-charged wormhole solution and $(\rho^{(1)}, p_1^{(1)})$ are the charged dressing,

$$\rho^{(1)} = -p_1^{(1)} = \frac{Q^2}{8\pi r^4},\tag{7.2}$$

where Q is the electric charge. As one can see in the above equation (7.1), $p_1 \neq -\rho$ or $w_1 \neq -1$ unless $\rho^{(0)} = p_1^{(0)} = 0$. As the authors pointed out in the paper, it corresponds to the $b(r) = 0$ case in the reference. and the spacetime becomes the Reissner-Nordström solution.

One may also use our solutions to make a new solution which use exotic matter minimally. In the vicinity of the ‘throat’, the truncated solution of us can be matched with a Schwarzschild one outside with appropriate junction conditions [18]. Stability of wormholes has also been studied in part in the context of general relativity recently [25, 26]. Though the studies are not yet complete, it was shown that the Ellis type wormhole can be stable at least. As the stability of a black hole made physicist to consider black hole seriously, we expect the stability of a wormhole do the role.

Most studies of wormhole concentrate on finding a solution of the gravitational field equations. Recently the exact form of entropy function $S(r)$ for a self-gravitating anisotropic matter was obtained [27]. When a wormhole is made of an anisotropic matter of radius R and the ‘throat’ radius is B , the entropy is given by a sum of $S_1(R) - S_1(B)$ in one side and $S_2(R) - S_2(B)$ in the other side of the wormhole. Though there have been a few studies, the wormhole thermodynamics, should be addressed to have more clear picture.

In this work, we cannot avoid the use of exotic matter because we are based on the general relativity. The extension of the analysis to a modified theory of gravity is admirable.

Acknowledgments

This work was supported by the National Research Foundation of Korea grants funded by the Korea government NRF-2017R1A2B4008513.

References

- [1] M. S. Morris and K. S. Thorne, *Am. J. Phys.* **56** (1988) 395. doi:10.1119/1.15620
- [2] M. S. Morris, K. S. Thorne and U. Yurtsever, *Phys. Rev. Lett.* **61** (1988) 1446. doi:10.1103/PhysRevLett.61.1446
- [3] S. W. Kim and H. Lee, *Phys. Rev. D* **63** (2001) 064014 doi:10.1103/PhysRevD.63.064014 [gr-qc/0102077].
- [4] A. Raychaudhuri, *Phys. Rev.* **98** (1955) 1123. doi:10.1103/PhysRev.98.1123
- [5] V. P. Frolov and I. D. Novikov, *Phys. Rev. D* **42** (1990) 1057. doi:10.1103/PhysRevD.42.1057
- [6] C. W. Misner and J. A. Wheeler, *Annals Phys.* **2** (1957) 525. doi:10.1016/0003-4916(57)90049-0
- [7] H. C. Kim and Y. Lee, arXiv:1902.02957 [gr-qc].
- [8] H. B. G. Casimir, *Indag. Math.* **10** (1948) 261 [Kon. Ned. Akad. Wetensch. Proc. **51** (1948) 793] [Front. Phys. **65** (1987) 342] [Kon. Ned. Akad. Wetensch. Proc. **100N3-4** (1997) 61].
- [9] L. H. Ford and T. A. Roman, “Negative energy, wormholes and warp drive,” *Sci. Am.* **282N1** (2000) 30.
- [10] K. A. Bronnikov and V. G. Krechet, arXiv:1807.03641 [gr-qc].
- [11] M. R. Mehdizadeh, M. Kord Zangeneh and F. S. N. Lobo, *Phys. Rev. D* **91** (2015) 084004. doi:10.1103/PhysRevD.91.084004 [arXiv:1501.04773 [gr-qc]].
- [12] M. Kord Zangeneh, F. S. N. Lobo and M. H. Dehghani, *Phys. Rev. D* **92** (2015), 124049. doi:10.1103/PhysRevD.92.124049 [arXiv:1510.07089 [gr-qc]].
- [13] S. H. Mazharimousavi and M. Halilsoy, *Mod. Phys. Lett. A* **31** (2016) no.34, 1650192. doi:10.1142/S0217732316501923
- [14] K. K. Nandi, A. Islam and J. Evans, *Phys. Rev. D* **55** (1997) 2497 doi:10.1103/PhysRevD.55.2497 [arXiv:0906.0436 [gr-qc]].
- [15] E. F. Eiroa, M. G. Richarte and C. Simeone, *Phys. Lett. A* **373** (2008) 1 Erratum: [Phys. Lett. **373** (2009) 2399] doi:10.1016/j.physleta.2008.10.065, 10.1016/j.physleta.2009.04.065 [arXiv:0809.1623 [gr-qc]].
- [16] J. Maldacena and L. Susskind, *Fortsch. Phys.* **61** (2013) 781 doi:10.1002/prop.201300020 [arXiv:1306.0533 [hep-th]].
- [17] J. Maldacena, A. Milekhin and F. Popov, arXiv:1807.04726 [hep-th].
- [18] W. Israel, *Nuovo Cim. B* **44S10** (1966) 1 [Nuovo Cim. B **44** (1966) 1] Erratum: [Nuovo Cim. B **48** (1967) 463]. doi:10.1007/BF02710419, 10.1007/BF02712210
- [19] M. Visser, Woodbury, USA: AIP (1995) 412 p
- [20] H. C. Kim, *Phys. Rev. D* **96**, no. 6, 064053 (2017) doi:10.1103/PhysRevD.96.064053 [arXiv:1708.02373 [gr-qc]].
- [21] I. Cho and H. C. Kim, *Phys. Rev. D* **95**, no. 8, 084052 (2017) doi:10.1103/PhysRevD.95.084052 [arXiv:1610.04087 [gr-qc]].
- [22] I. Cho and H. C. Kim, arXiv:1703.01103 [gr-qc].

- [23] S. Halder, S. Bhattacharya and S. Chakraborty, Phys. Lett. B **791** (2019) 270 doi:10.1016/j.physletb.2019.02.041 [arXiv:1903.03343 [gr-qc]].
- [24] R. D. Sorkin, R. M. Wald and Z. J. Zhang, Gen. Rel. Grav. **13**, 1127 (1981).
- [25] K. A. Bronnikov, L. N. LipTOVa, I. D. Novikov and A. A. Shatskiy, Grav. Cosmol. **19** (2013) 269 doi:10.1134/S0202289313040038 [arXiv:1312.6929 [gr-qc]].
- [26] I. Novikov and A. Shatskiy, arXiv:1201.4112 [gr-qc].
- [27] H. C. Kim and Y. Lee, arXiv:1901.03148 [hep-th].